

# Sensorless Control of Salient Pole PMSM Using a Low-Frequency Signal Injection

Matti Eskola, Heikki Tuusa  
Tampere University of Technology  
P.O. Box 692 FI-33101  
Tampere, Finland  
Tel.: +358 3 311 511  
Fax: +358 3 3115 2088  
E-Mail: matti.eskola@tut.fi  
URL: <http://www.tut.fi>

## Keywords

Permanent magnet motor, sensorless control

## Abstract

This paper deals with sensorless control of permanent magnet synchronous motor. The low-frequency signal injection estimator is studied in the case of salient PMSM. If there is an error in the estimated position, the injected signal creates a torque oscillation and affects the back-emf. The oscillating back-emf can be used to track the position and speed. The saliency of the PMSM is a disturbance for the low frequency estimator. In this paper the effect of saliency is analysed in steady state and a simple method to compensate the saliency effect is proposed. The performance of the method is verified by measurements.

## Introduction

Sensorless control systems using the fundamental frequency motor model [1]-[3] perform well in speed range over 5-10 % of nominal speed. The zero and low speed regions are problematic because the information on the rotor angle is lost when the angular speed approaches zero. The fundamental frequency model based estimators also need information on PMSM parameters:  $R$ ,  $L$  and  $\psi_m$ . If the parameters are not accurately known the performance of the control system deteriorates at higher speeds, too. During the last ten years extensive research has been carried out to develop estimators to avoid these problems at low speeds. The methods suitable for zero speed operation are called "injection methods". In most of these methods high frequency voltage signal is injected into the motor and the position angle and speed are determined by processing the resulting voltages or currents. These estimators exploit the magnetic saliency ( $L_d < L_q$ ) of the PMSM. A number of high frequency (HF) signal injection variants has been reported [4]-[7].

A low-frequency signal injection method has recently been introduced for induction motors [8]. This estimator method is also stable at zero speed and gives a smooth torque. The slow dynamics is the drawback of this estimator. At higher speeds it should be used with a model based estimator [8].

The low frequency estimator can be applied also in the case of PMSM. A low frequency current component is injected in the direction of the permanent magnet flux (d-axis). If the estimate of the angle is not correct there is also a torque producing quadrature axis component, which causes a mechanical oscillation. Oscillation can be detected from currents and voltage reference signals provided that the inertia is not too high. This signal is used to drive the position error to zero. The low-frequency estimator uses the motor model but it is somewhat insensitive to parameter errors.

In [9] the low frequency method is analysed in the case of symmetric PMSM ( $L_d = L_q$ ) and tested only by simulations. The PMSM is salient if  $L_d < L_q$ . This is the case with interior magnet PMSMs and also

with surface magnet machines because the strong magnets saturate the stator iron in the direction of the flux. The saliency of the motor is a distortion for the low-frequency estimator method. Thus the basic idea is quite different compared to the high frequency methods, where the saliency is a necessary condition for the estimator. The effect of the saliency of the PMSM has not been discussed earlier in the literature in the case of low-frequency injection. In this paper the effect of saliency is analysed theoretically and verified by measurements. A simple compensation method to prevent large steady state position errors is proposed.

## Signal injection using a low frequency carrier signal

The fundamental frequency voltage model of the PMSM can be written in synchronous reference frame as follows:

$$\begin{aligned} u_d &= R i_d + L_d \frac{di_d}{dt} - \omega_r L_q i_q \\ u_q &= R i_q + L_q \frac{di_q}{dt} + \omega_r (\psi_m + L_d i_d) \end{aligned} \quad (1)$$

Where  $\psi_m$  is the PM flux. In the low frequency injection estimator studied in this paper the sinusoidal low frequency signal is added to the d-axis current reference, Fig. 1. In general case the d- and q-axis currents contain DC-components ( $i_d$  and  $i_q$ ) and sinusoidal components ( $i_{cd}$  and  $i_{cq}$ ) with injection frequency  $\omega_c$ . The equation of the torque and the equation of motion are

$$T_e = 3p/2 (\psi_m (i_q + i_{cq}) + (\Delta L)(i_d + i_{cd})(i_q + i_{cq})) \quad (2)$$

$$\omega_r = \frac{p}{J} \int (T_e - T_{Load}) dt \quad (3)$$

In (2)  $\Delta L = L_d - L_q$ . The basic idea of the low frequency method is first explained by assuming the completely non-salient machine,  $\Delta L = 0$  [9]. In that ideal case the torque produced by the PMSM is a function of q-axis current only. If the estimated position angle of the rotor is not correct the sinusoidal current is also injected in q-axis direction which causes mechanical oscillation. The sinusoidal q-axis current component with frequency  $\omega_c$  is approximately

$$i_{cq} \approx -i_{cd}^* \sin \tilde{\theta} \quad (4)$$

where  $\tilde{\theta}$  is the position error  $\theta - \hat{\theta}$ .  $\hat{\cdot}$  denotes the estimated quantity. The transformation between the actual and estimated d,q frame is illustrated in Fig. 2a. (4) is substituted into (2). Using (3) it is possible to write expression for a back-emf:  $e_q = -\omega_r \psi_m$ . The load torque is assumed to be constant. The back-emf calculated by (3) is in the actual d,q-reference frame. To get the expression for the error signal the  $e_q$  must be transformed to the estimated reference frame with angle  $\hat{\theta}$ . The average component of the  $e_q$  is omitted because only the oscillating component  $e_{cq}$  is interesting when the low frequency injection method is analysed. If d-axis current reference signal is  $I_c \cos(\omega_c t)$ , Fig. 1, the estimated back-emf component in control systems reference frame is [9]

$$\hat{e}_{cq} = \cos \tilde{\theta} \sin \tilde{\theta} \frac{3p^2 \psi_m^2 I_c}{J \omega_c} \sin(\omega_c t) \approx \tilde{\theta} \frac{3p^2 \psi_m^2 I_c}{J \omega_c} \sin(\omega_c t) \quad (5)$$

It can be seen from (5) that the amplitude of the oscillating back-emf  $\hat{e}_{cq}$  is proportional to inertia  $J$  and number of pole pairs  $p$ . If  $J$  is too high this estimator method cannot be applied.

## Estimator structure

The estimate of the oscillating back-emf in the q-direction (5) is obtained using the basic voltage equation in synchronous reference frame (1), Fig. 1. Estimated parameters and estimated speed are used in the algorithm. The reference signals of voltage and current are used instead of the actual values. This is done to decrease the noise in the system.



$$\omega_r = \omega_{r0} + \omega_{cr} = \omega_{r0} + \frac{p}{J} \int T_{ce} dt = \omega_{r0} + \underbrace{\frac{3p^2}{2J} \int (\psi_m i_{cq} + \Delta L (i_d i_{cq} + i_q i_{cd})) dt}_{\omega_{cr}}, \quad (10)$$

where  $\omega_{c0}$  is average speed and  $\omega_{cr}$  is the oscillating speed with frequency  $\omega_c$ . Now we can write the voltage equations in actual synchronous reference frame. Only the oscillating components with frequency  $\omega_c$  are included.

$$\begin{aligned} u_{cd} &= R i_{cd} + L_d \frac{di_{cd}}{dt} - L_q (\omega_{r0} i_{cq} + \omega_{cr} i_q) \\ u_{cq} &= R i_{cq} + L_q \frac{di_{cq}}{dt} + L_d (\omega_{r0} i_{cd} + \omega_{cr} i_d) + \psi_m \omega_{cr} \end{aligned} \quad (11)$$

Using (8) – (11) we can build a model in a more convenient form for the steady state analysis of the low frequency estimator, Fig. 2b. This model contains the current control, PMSM and the block calculating the estimate of the oscillating back-emf  $\hat{e}_{cq}$ . The  $\hat{e}_{cq}$  block of Fig. 1 is simplified by neglecting the derivative of  $i_q$ . This can be done because the steady state performance is analysed and the  $i_q$  reference contains no component with frequency  $\omega_c$ . For the same reason the speed control is not included.

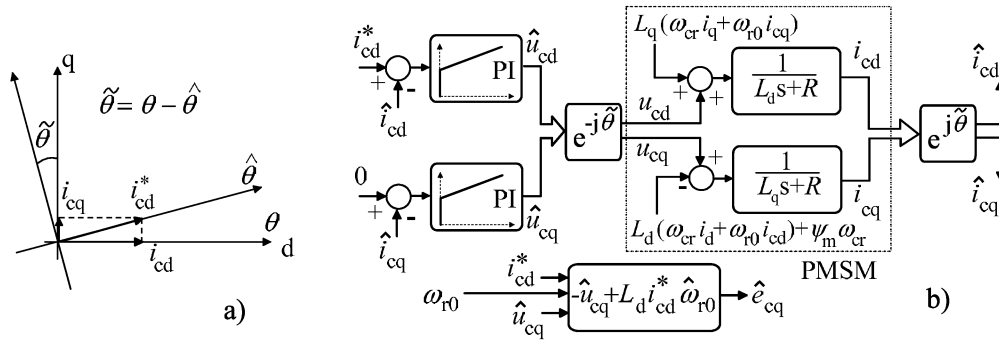


Fig. 2: a) Transformation between the actual and estimated d,q-frame. b) Simplified structure of the control system and low frequency estimator.

Using Fig. 2b it is possible to write a transfer function between the estimated back-emf and  $i_{cd}$  reference.

$$G_e(s) = \frac{\hat{e}_{cq}(s)}{i_{cd}^*(s)} = \frac{-(K_p s + K_i)^2 \left( \frac{\Delta L \sin(2\tilde{\theta})}{2} s^2 + \omega_{r0} (L_d \cos^2 \tilde{\theta} + L_q \sin^2 \tilde{\theta}) s + A \right)}{(L_d L_q s^4 + (K_p + R)(L_d + L_q) s^3 + B s^2 + C s + D) s} + \hat{L}_d \omega_{r0} \quad (12)$$

where

$$\begin{aligned} A &= -\frac{3p^2 \sin(2\tilde{\theta})}{4J} (\Delta L (\psi_q i_q + \psi_d i_d) + \psi_m \psi_d) + \frac{3p^2}{2J} (\psi_q \sin^2 \tilde{\theta} (\psi_m + \Delta L i_d) + \Delta L \psi_d i_q \cos^2 \tilde{\theta}) \\ B &= \left( \omega_{r0}^2 L_d L_q + (K_p + R)^2 + K_i (L_d + L_q) + \frac{3p^2}{2J} (\psi_m \psi_d L_d + \Delta L \psi_d L_d i_d - \Delta L \psi_q L_q i_q) \right) \\ C &= (K_p + R) \left( 2K_i + \frac{3p^2}{2J} (\psi_m \psi_d - \Delta L \psi_q i_q + \Delta L \psi_d i_d) \right) + \frac{\omega_{r0} 3p^2}{2J} (\Delta L (\psi_d L_q i_q + \psi_q L_d i_d) + L_d \psi_m \psi_q) \\ D &= K_i^2 + \frac{3p^2 K_i}{2J} (\Delta L \psi_d i_d - \Delta L \psi_q i_q + \psi_m \psi_d) \end{aligned}$$

In (12)  $K_p$  is the gain of the PI controller and  $K_i$  is the gain  $K_p$  divided by the integration time  $T_i$ .  $\psi_d$  and  $\psi_q$  are DC components of the flux ( $\psi_m + L_d i_d$  and  $L_q i_q$ ).

If the rotor speed is near zero and the PI controllers are very fast the denominator of (12) approaches  $s(K_{ps} + K_i)^2$ . If this approximation is used and only the injection frequency is taken into account we can write a simplified expression for the gain and phase of (12).

$$\begin{aligned} \text{Gain}(G_e(s)) &\approx \sqrt{\omega_{r0}^2 (L_d \cos^2 \tilde{\theta} + L_q \sin^2 \tilde{\theta})^2 + \left( -\frac{\Delta L \sin(2\tilde{\theta})}{2} \omega_c + \frac{A}{\omega_c} \right)^2} \\ \text{Phase}(G_e(s)) &\approx \tan^{-1} \left( \frac{\left( -\frac{\Delta L \sin(2\tilde{\theta})}{2} \omega_c + \frac{A}{\omega_c} \right)}{-\omega_{r0} (L_d \cos^2 \tilde{\theta} + L_q \sin^2 \tilde{\theta})} \right) \end{aligned} \quad (13)$$

The coefficient  $A$  is same in (12) and (13). Compared to (12) the simplified model (13) does not take the tuning of the PI controllers into account. If injection frequency  $\omega_c$  is high the accuracy of (13) decreases because the  $s^4$  and  $s^3$  components of the denominator of (12) are omitted.

### Zero speed analysis

First the position error related to the saliency is analysed at zero speed,  $\omega_{r0} = 0$  (12), (13). The low frequency estimator, Fig. 1, stabilizes to the operating point where the gain of (12) is zero. In that case the  $\hat{e}_{cq}$  is zero and the PLL algorithm, Fig. 1, does not change the estimated rotor position.

First the position error is assumed to be zero. The only nonzero component in the gain (13) is  $3p^2 \Delta L \psi_{diq} / 2J$  inside the coefficient  $A$ . The phase shift is approximately  $-\pi/2$  (13). In the demodulation process, Fig. 1,  $\hat{e}_{cq}$  is multiplied by a signal with  $-\pi/2$  phase lag compared to  $i_{cd}^*$ . Thus the  $\hat{e}_{cq}$  has a non-zero amplitude and it is in phase with demodulation signal. The error signal  $\varepsilon_\theta > 0$ . The estimated position increases. The next important operating is the position error where the torque oscillation with frequency  $\omega_c$  is zero. This is the case when the coefficient  $A$  (12),(13) is zero. If the current controllers, Fig 2b, are assumed to be fast the sinusoidal current components with frequency  $\omega_c$  are approximately

$$i_{cd} \approx i_{cd}^* \cos \tilde{\theta} + i_{cq}^* \sin \tilde{\theta}, \quad i_{cq} \approx -i_{cd}^* \sin \tilde{\theta} + i_{cq}^* \cos \tilde{\theta} \quad (14)$$

Now the  $i_{cq}$  reference is zero. When (9) and (14) are substituted into expression of  $\omega_{cr}$  (10) we can write an expression for position error which gives zero oscillation with frequency  $\omega_c$ .

$$\tilde{\theta}_{zo} \approx \tan^{-1} \left( \frac{\psi_m - \sqrt{\psi_m^2 + 4\Delta L^2 i_q^2}}{-2\Delta L i_q} \right). \quad (15)$$

However, the position estimate still increases because the saliency dependent coefficient  $-\Delta L \sin(2\tilde{\theta}) < 0$  (13). The coefficient  $A$  is positive if  $\tilde{\theta} < \tilde{\theta}_{zo}$ .

Finally the position error stabilizes when  $-0.5\Delta L \sin(2\tilde{\theta}) \omega_c^2 + A = 0$  (13). If the gain of the transfer function (13) is simplified by neglecting all coefficients 10 times smaller compared to the largest one the following expression can be written for position error in steady state.

$$\tilde{\theta}_{ss} \approx \tan^{-1} \left( \frac{-2J\Delta L \omega_c^2 - 3p^2 \psi_m^2 + \sqrt{4\Delta L^2 \omega_c^4 J^2 + 3p^2 \psi_m^2 (4\Delta L \omega_c^2 J + 3p^2 \psi_m^2 + 12p^2 \Delta L^2 i_q^2)}}{6p^2 \Delta L \psi_m i_q} \right) \quad (16)$$

Steady state position error as a function of saliency, inertia, injection frequency and the load are illustrated in Fig. 3. The parameters are from Table I. The inertia used in the simulations of Fig. 3 is not from Table I. In Fig. 3  $J$  is  $17.5 \text{ kgm}^2$  which is the inertia of the drive seen by the estimator. This is

explained in the Experimental tests section. The results achieved by (12) and a simplified case (16) are compared to the results from the full Simulink model with speed control loop. Fig. 3 shows that the simple model (13), (16) gives accurate results if the position error is smaller than  $15^\circ$ . The analysis shows that quite small saliencies can lead to significant steady state errors in position. Thus the effect of saliency must be compensated.

### Effect of speed

In Fig. 3 angular speed  $\omega_{r0}$  is assumed to be zero or very small. If the speed is nonzero it interacts with  $i_{cd}$  and  $i_{cq}$  (11). The  $\omega_{r0}i_{cd}$  is the dominant component and causes a sinusoidal q axis current. The current controller tries to compensate it ( $i_{cq}$  reference = 0). If the PI controller, Fig. 2, is not extremely fast there will remain some sinusoidal voltage, which causes an additional error to  $\hat{e}_{cq}$  (12). It can also be seen from (13) that non-zero  $\omega_{r0}$  changes the amplitude and phase shift of  $\hat{e}_{cq}$ . Contrary to the zero speed case the steady state error is now clearly dependent on the tuning of the current control. Thus the simple model (13) gives accurate results only if speed  $\omega_{r0}$  is zero or very slow. Fig. 4. shows the error when the speed varies from -10% to 10% speed. The results are calculated with three  $T_i$  using (12). If  $T_i$  is kept constant and  $K_p$  varies the results are almost similar. Increased inertia and saliency increase the speed dependent error. However, this speed dependent error also exists when the PMSM is symmetric ( $L_d = L_q$ ). If current control is tuned fast enough and the low frequency method is used only at low speeds it is not necessary to compensate the speed effect.

### Effect of parameter errors in steady state

The low frequency estimator needs the motor model although it is a signal injection method. However, in steady state the parameter errors are unsubstantial. This is especially the case when there is no q axis current reference signal with frequency  $\omega_c$ , Fig. 1. This can be seen from (6) and Fig. 2. If  $i_q$  reference contains no injection frequency component, errors in  $L_q$  and  $R$  have no effect on steady state error. If  $\omega_r \neq 0$ ,  $L_d$  is still included in the equation of back-emf, Fig. 2. The effect of  $L_d$  error was analysed using (12).  $\pm 50\%$  errors cause only minimal changes to the steady state position error (within  $\pm 0.2^\circ$ ), Fig. 5, when the speed of the PMSM is changed from -10% to 10% speed. However, the parameter errors are not negligible when the transient performance is studied.

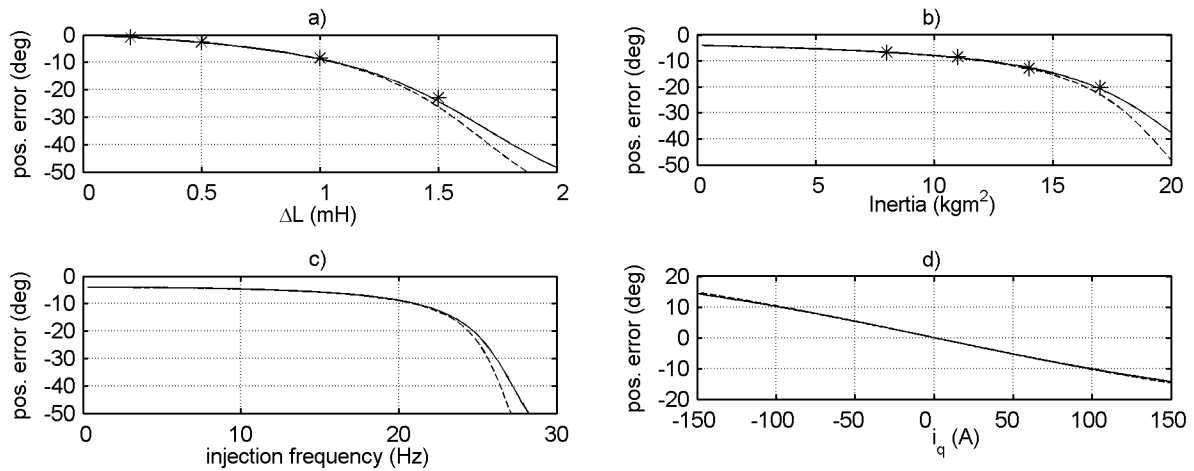


Fig. 3: Zero speed steady state position error  $\theta - \hat{\theta} = \tilde{\theta}$  of the PMSM of Table I. In a)  $\Delta L$  varies while other parameters and load is nominal. In b), c) and d) variable quantities are inertia, injection frequency and  $i_q$  respectively. The steady state error is calculated by (12) (solid line) and (16) (dashed line). Results from the full model are marked by \*.

### Effect of drive disturbances

In addition to the saliency of the PMSM the estimated speed and position are also affected by measurement errors, non-linear effects of the inverter bridge and additional saliencies of the PMSM. These properties of the real drives cause periodic disturbances to the position and speed estimate signal. The disturbances caused by measurements and inverter bridge are well known and have been

widely studied in the literature [10]. Every time one of the phase currents crosses zero the error voltage vector caused mainly by the dead times of the inverter bridge changes. This creates 6<sup>th</sup> harmonic to the estimated quantities if it is not compensated. Accurate compensation requires that dead times and voltage losses in switches are known. Offset errors and unbalanced gains in the current measurement system cause oscillation to the estimated quantities with frequency  $\omega_r$  and  $2\omega_r$  [10].  $\omega_r$  is the fundamental supply frequency of the PMSM.

The other source of periodic disturbance is the PMSM itself [11],[12]. In the case of a real motor the phase inductances are not perfectly sinusoidal functions of the rotor angle. This means that  $\Delta L$  is a function of the rotor position. There also exists additional harmonic components in the rotor flux linkage which can cause a torque ripple [11]. The compensation of these machine related oscillations requires that the properties of the PMSM are known in detail. The compensation of disturbances caused by non-ideal properties of the PMSM drive are not analysed in this paper.

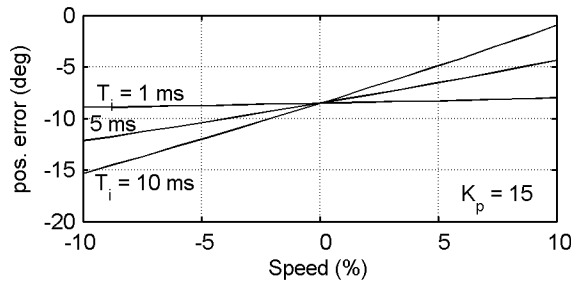


Fig. 4: Steady state position error as a function of speed. Load and the other parameters are nominal.

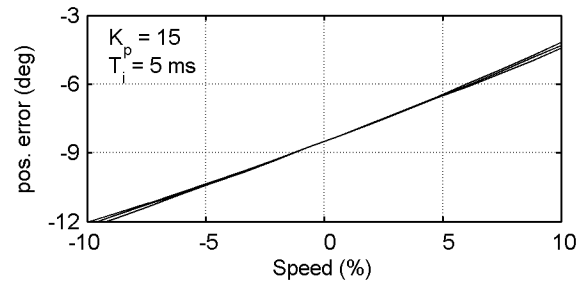


Fig. 5: Steady state position error.  $\hat{L}_d$  varies between 50% and 150%.

## Compensation of the steady state position error

Two methods to prevent large steady state error in position estimate are now presented. The first one is to drive the position error to value (15) where the oscillation in the torque with injection frequency is zero. This can be done by adding a compensating signal to the error signal  $\varepsilon_\theta$ , Fig. 1. This signal is half of the  $\hat{e}_{cq}$  amplitude when the position error is  $\tilde{\theta}_{zo}$  (15). The exact value for the compensation signal can be found using (12). For on-line purposes (13) is used.

$$c = \hat{e}_{cq} / 2 \approx -i_d^* \Delta L \omega_c \sin(2\tilde{\theta}_{zo}) / 4. \quad (17)$$

The compensating signal  $c$  is a function of  $i_q$  and it must be updated on-line if the load is not constant. In most cases  $\tilde{\theta}_{zo}$  can be approximated to be linearly dependent on  $i_q$ . Thus (17) can be simplified:  $c = \text{constant} * i_q$  if angle (15) is fairly small ( $< 8^\circ$ ). In simulations the steady state angle error (15) compared to the theoretical error was smaller than  $0.6^\circ$  when (17) was used as a compensation signal.

The other compensation method is also to inject a convenient low frequency signal in the q-axis direction. The idea is to cancel the reluctance component from the equation of the torque. If (14) is substituted into the equation of the torque (2) it can be found that there is no oscillation in the rotor speed with frequency  $\omega_c$  if the position error is zero and

$$i_{cq}^* = -i_{cd}^* i_{q\psi_m}^{-1} \Delta L \quad (18)$$

The reference signal in q-direction is in phase with the main injection signal  $i_{cd}^*$  and its amplitude is proportional to the saliency ratio, PM flux constant and the load. Even if the position error is not zero the injection of (18) compensates the effect of the reluctance torque with good accuracy. Injecting (18) the steady state position error in theory is zero. In practice the non-ideal current controllers cause a small error. However, the saliency ratio, inertia and other parameters restrict the use of this compensation method. Even if injecting (18) removes the other coefficients with  $\Delta L$  from the numerator of (12) there exists a component  $0.5\Delta L \sin(2\tilde{\theta})$ . If it increases faster than coefficient  $A$

(12),(13) when the position error increases the system is unstable or at least the steady state error becomes considerable. If the slope of these coefficients (13) are studied around the zero position error the following condition can be written for the inertia and saliency  $\Delta L$ .

$$\Delta L \omega_c^2 + \frac{3p^2 \psi_m^2}{2J} > 0 \quad (19)$$

**Table I: Parameters and nominal values of the PMSM drive.**

$R$	$L_d, L_q$	$J$	Pole pairs	$\psi_m$	$\omega_r$	$I$ (RMS)
0.3 $\Omega$	8.5, 9.5 mH	Drive: 33 kgm <sup>2</sup>	12	1.2 Wb	148 rad/s, 117.6 rpm (mech.)	60 A
Speed controller		Current controller		Estimator PLL		$i_d$ reference (carrier)
$K_p = 2, T_i = 65$ ms		$K_p = 16, T_i = 9$ ms		$K_p = 5, T_i = 0.5$ s		13 A, 20 Hz

## Experimental tests

The motor used in the experimental tests is a 23 kW axial flux machine, Fig. 6. The parameters and nominal values of the motor are introduced in Table I. The PMSM used in experimental tests is challenging for the low frequency method as far as the inertia is concerned. On the basis of Fig. 3 it seems to be almost impossible to apply the low frequency estimator with this PMSM if total inertia of the drive is 33 kgm<sup>2</sup>. In this paper the power transmission between the PMSM and DC-machine is implemented with a cogged belt. Thus the connection between machines is slightly elastic. This allows the adequate oscillation for the rotor. Fig. 7. shows the measured position error when the speed is 2% of nominal and the load is 65%. The effect of saliency is not compensated. From the estimator's point of view the inertia is now approximately 17.5 kgm<sup>2</sup> (16).

## Control board and test bench

Implementation of the control system, estimator algorithms and the modulator were carried out using the Motorola MPC555 microprocessor. The measured signals were phase currents and the voltage of the DC bus of the inverter. A/D conversions were performed by MPC555's 10 bit A/D converters. All algorithms were implemented using only fixed point operations. This allowed us to calculate the control, PWM modulation and estimator algorithms all in 100  $\mu$ s loop. All software procedures were written in C language. The most critical operations were written in Assembly language. The PMSM was fed by a voltage source inverter where the 400 V line voltage was rectified by a diode bridge. The load of the PMSM was a 50 kW DC-machine, Fig. 6.

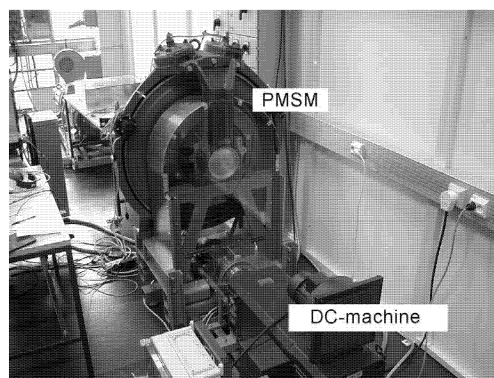


Fig. 6: The test bench.

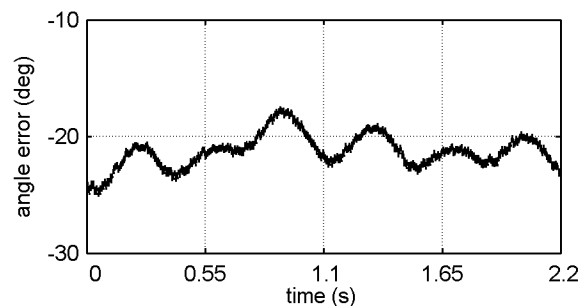


Fig. 7: Measured position error. 2% speed, 65% load. The effect of saliency is not compensated.

## Experimental results

In Fig. 8 speed is 2% and the load is nominal. Now the sinusoidal signal is also injected in the q-axis direction (18). The average position error is approximately zero and the maximum error is smaller than 5° (electric position). The measured speed is shown in Fig. 8b. The 6<sup>th</sup> harmonic is the dominant



component, Fig. 8c. The 6<sup>th</sup> harmonic is caused mainly by inverter bridge dead times and non-ideal motor structure. No attempt is made in this paper to compensate the additional saliencies. 20 Hz injection signal can be seen in Fig. 8d which shows the measured phase currents. The injection frequency can be found also from the measured speed, 42<sup>th</sup> harmonic in Fig. 8c. Thus there exists some oscillation with injection frequency  $\omega_c$  because the position error is not zero all the time.

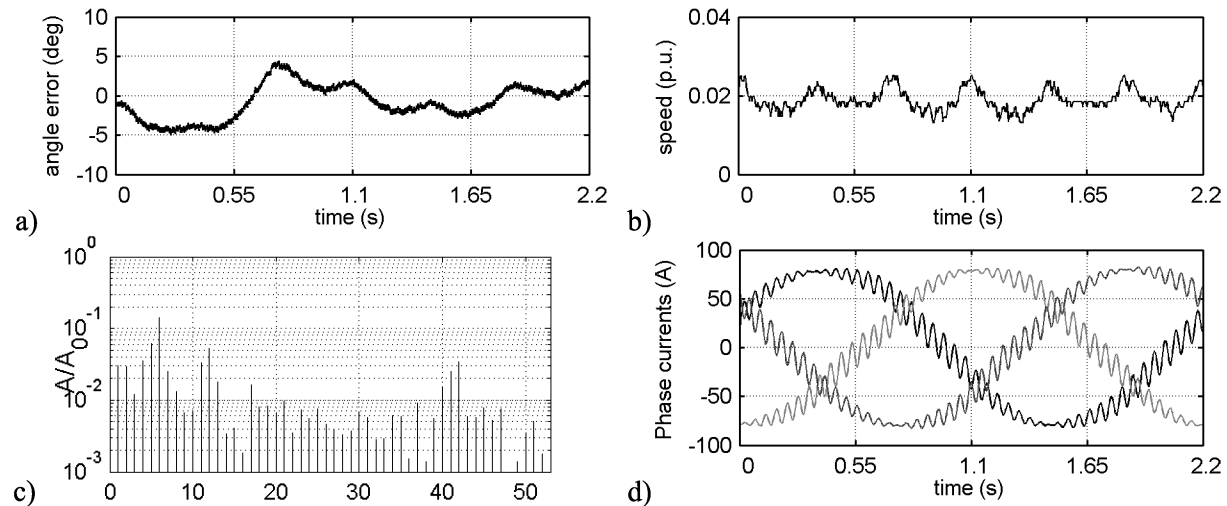


Fig. 8: Steady state test. The load is nominal and the speed is 2%. a) measured position error, b) measured angular speed, c) frequency spectrum of the angular speed, d) phase currents. The effect of the saliency is compensated using (18).

Fig. 9 shows the measured position error and angular speed when the speed reference is changed from 4% speed to -4% speed. When the speed is negative the PMSM regenerates. If the reference ramp is rather slow, Fig. 9, there are no stability problems. In Fig. 10 the speed reference is zero and the load is changed suddenly from zero to 30% of nominal. Now the position error during the transient is significant. If the load step test is performed with 50% load the stability of the drive is lost.

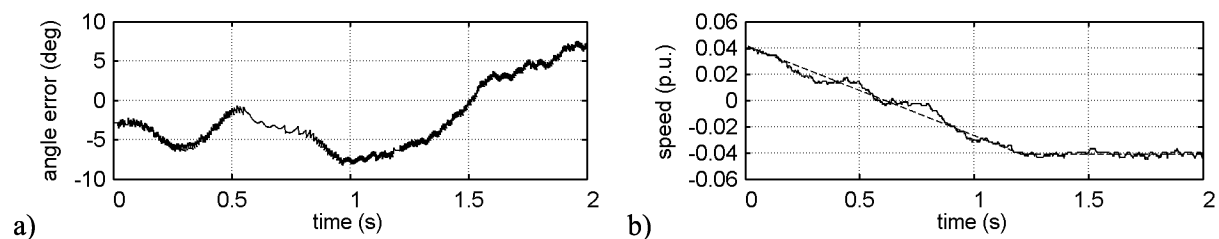


Fig. 9: Speed reversal from motoring to regenerative region. a) Measured position error, b) measured speed (solid line), reference signal (dashed line).

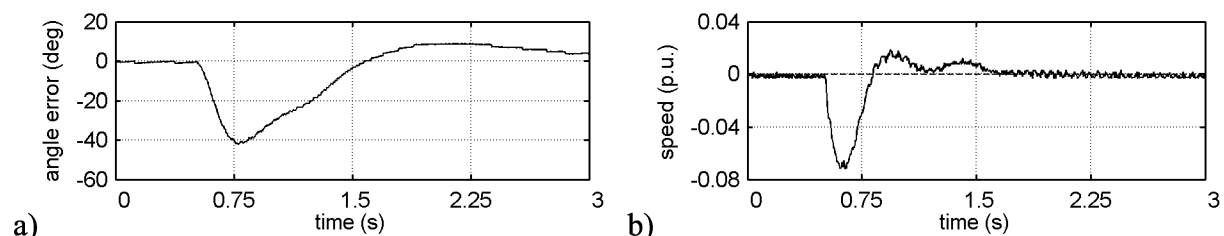


Fig. 10: Load step from 0 to 30%. a) measured position error, b) measured speed (solid line), speed reference (dashed line).

## Conclusions

This paper presented a PMSM drive where the rotor position and angular speed were estimated using the low frequency signal injection method. The saliency of the PMSM can be considered to be a disturbance when the low frequency method is applied. The effect of saliency was analysed in steady

state operation. It was found that rather small saliencies can lead to significant estimation errors. The simple method of compensating this disturbance was introduced for the PMSM drive.

The applicability of this method was confirmed in experimental tests. The sensorless control system was stable at low speed region and the compensation of the saliency effect was successful. The dynamics of the estimator is rather poor due to the low injection frequency. If this method is used in practice the injection method should be assisted by some simple model based estimator [8]. Using a hybrid estimator the dynamic performance is improved and operation at higher speed is possible.

## References

- [1] Lawrence A. Jones and Jeffrey H. Lang, A State observer for the permanent magnet synchronous motor, IEEE Transactions on industrial electronics, Vol. 36, No. 3, August 1989.
- [2] Lennart Harnefors, Magnus Jansson, Rolf Ottersten and Kai Pietiläinen, Unified sensorless vector control of synchronous and induction motors, Industrial Electronics, IEEE Transactions on Industrial Electronics, Volume 50, Issue 1, Feb. 2003, pp. 153 – 160.
- [3] Li Ying and Nesimi Ertugrul, A novel, robust DSP-based indirect rotor position estimation for permanent magnet AC motors without rotor saliency, IEEE Transactions on Power Electronics Volume 18, No. 2, March 2003, pp. 539 – 546.
- [4] Manfred Schrödl, Michael Lambeck and Ewald Robeischl, "Implementation of the INFORM method in a commercial converter for sensorless PM synchronous drives," International Conference on Power Electronics, Intelligent Motion, Power Quality (PCIM) 2002.
- [5] Matthew. J. Corley and Robert D. Lorenz, "Rotor position and velocity estimation for a salient-pole permanent magnet synchronous machine at standstill and high speeds," Industry Applications, IEEE Transactions on, Volume: 34 , Issue: 4, 1998, pp. 784 – 789.
- [6] Marco Linke, Ralph Kennel and Joachim Holtz, "Sensorless position control of permanent magnet synchronous machines without limitation at zero speed," 28<sup>th</sup> Annual Conference of the IEEE industrial Electronics Society IECON'02, Sevilla/Spain, Nov. 5-8, 2002.
- [7] Cesar Silva, Greg M. Asher, Mark Sumner and Keith J. Bradley, Sensorless control in a surface mounted PM machine using rotating injection, EPE Journal, Vol. 13, No. 3, August 2003.
- [8] Veli-Matti Leppänen, A Low-Frequency signal-injection method for speed sensorless vector control of induction motors, Thesis for the degree of doctor of science in technology, Helsinki university of technology, Institute of intelligent power electronics, Espoo, 2003.
- [9] Tamas Kereszty, Veli-Matti Leppänen and Jorma Luomi, Sensorless control of surface magnet synchronous motors at low speeds using low-frequency signal injection, Conference record of the 29<sup>th</sup> annual conference of the IEEE industrial electronics society, IECON'03, Roanoke, VA, 2-6, November 2003, pp. 1239-1243.
- [10] Joachim Holtz, Sensorless control of induction motor drives, Proceedings of the IEEE Volume 90, Issue 8, Aug. 2002, pp. 1359 – 1394.
- [11] Joachim Holtz and Lothar Springob, Identification and compensation of torque ripple in high-precision permanent magnet motor drive, IEEE Transactions on Industrial Electronics, Vol. 43, No. 2, April 1996. pp. 309-320.
- [12] Vladan Petrovic and Aleksandar M. Stankovic, Modeling of PM synchronous motors for control and estimation tasks, Proceedings of the 40th IEEE conference on decision and control, Orlando, Florida USA, December 2001.